A WIRELESSLY CONTROLLED SHAPE-MEMORY-ALLOY MEMS GRIPPER MICROFABRICATED USING AN ELECTROPLATING-BASED BONDING PROCESS

M. S. Mohamed Ali [1, 2*] *and K. Takahata* [1]
[1] The University of British Columbia, Vancouver, Canada
[2] Universiti Teknologi Malaysia, Skudai, Johor, Malaysia

ABSTRACT

This paper reports the wireless control of bulk-micromachined shape-memory-alloy actuators using an external radiofrequency magnetic field and its application to a MEMS gripper. The frequency-sensitive wireless resonant heater to which the gripper actuator is bonded is activated only when the field frequency is tuned to the resonant frequency of the heater. A bonding technique based on photo-defined copper electroplating is developed to mechanically and thermally couple the gripper with the planar heater circuit. The actuation range of 290 µm as the tip opening distance is obtained with normally-closed 4-mm-long grippers at a device temperature of 138 °C. The active frequency range is measured to be ~6 MHz. The manipulation of vertically aligned carbon nanotube forests is experimentally demonstrated.

INTRODUCTION

Bulk-micromachined shape-memory-alloy (SMA) actuators provide attractive features such as very large forces, high mechanical robustness with simple structures, and biocompatibility [1-3]. Various actuation mechanisms for SMA microactuators have been investigated. Joule heating by passing currents through heaters [4, 5] and directly through the SMA parts [6] is among the most widely used method to establish a heat source to the actuators. In this case, however, the mobility of the devices is severely constrained by the need of wired interface to them, limiting the application range for the devices. In order to address this, wirelessly controlled microactuators have been studied. For example, wireless SMA actuators in microrobotic applications were recently reported [7, 8]. However, they require batteries for their operations, resulting in relatively large device sizes and the need of complex control mechanisms. Nitinol, a biocompatible Ti-Ni alloy, has been expensively used in medical fields, enabling a variety of implantable devices and surgical tools [9-13]. Toward the application of SMA microactuators to this type of medical areas, the ability to wireless control is a key to reducing the interface complexity and hence promoting the practicality of the devices. In addition, passive configurations are highly beneficial to enable simple/robust, small, and low-cost products in these fields.

The reversible actuation of SMA has been approached mainly by two mechanisms – one-way memory assisted with external forces provided by cold-state reset layers [14] and two-way memory [15]. The one-way memory has been more commonly utilized for the actuation because of its reliability compared to the two-way memory approach that requires long thermal cycling for the material training and is not very stable. Despite of the favorable features of bulk SMA materials mentioned above, they have not been widely adopted in MEMS largely due to their incompatibility with standard batch microfabrication techniques and difficulties in their wafer-scale assembly. Recently, a wafer-scale integration method for bulk-SMA devices was reported [16]. However, polymer bonding utilized in the method poses issues in bonding quality and effective heat transfer to the SMA components. There are still many challenges in the integration of bulk SMA for MEMS applications.

This research explores a bulk-micromachined SMA-based microactuator that is passively controlled through radiofrequency (RF) power transfer to a wireless heater with which the SMA actuator is coupled. In order to address the issues related to SMA bonding, a planar assembly technique based on photo-defined selective electroplating is developed and used to bond the SMA actuators to the wireless heater circuits.

DEVICE PRINCIPLE

The micromachined SMA actuator developed in this effort is operated through an inductor-capacitor (LC) resonant circuit that serves as a frequency-sensitive wireless heater activated by an external RF magnetic field (Figure 1 (a)). An ac current is generated in an LC circuit when the circuit is exposed to an ac magnetic field due to the electromotive force induced by the field. The power consumed in the LC circuit, P, can be expressed as [17];

$$P(\omega) = \frac{Rv^2}{[R + j(\omega L - 1/\omega C)]^2} \quad (1)$$

where v is the electromotive force, L and C are respectively the inductance and the capacitance of the circuit, R is the parasitic resistance of the circuit, and ω is the angular frequency of the ac current. The reactance in (1) will be eliminated when the frequency of the ac current, or that of the magnetic field matches the resonant frequency of the circuit, $\omega_r = (LC)^{-1/2}$. At this condition, the power transfer to the circuit is maximized, resulting in:

$$P(\omega_r) = \frac{v^2}{R}\,. \quad (2)$$

Thus, the field energy is effectively converted to Joule heat when the field frequency is tuned to the resonant frequency of the LC circuit, i.e., the actuation is controlled with the frequency, rather than the field intensity. The steady state temperature rise of the LC circuit, T_{ss}, can be theoretically expressed as [18]:

$$T_{ss} = \frac{R_T v^2/R}{1 + \alpha_R R_T v^2/R} \quad (3)$$

where R_T is the thermal resistance to the surrounding of the circuit and α_R is the temperature coefficient of resistance of the circuit.

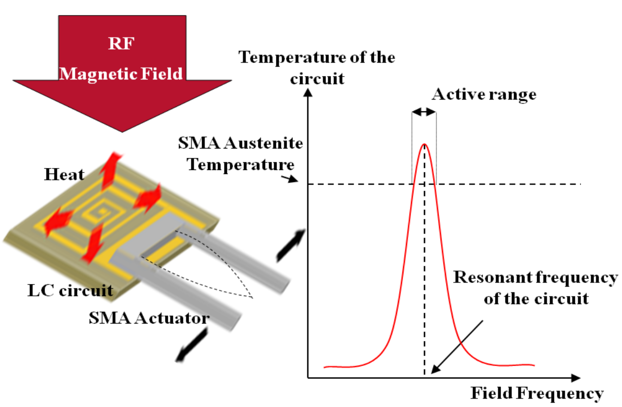

Figure 1: (a) Wirelessly controlled SMA micro-gripper and (b) working principle of the device.

The SMA gripper with two beams that have a rectangle cross section is fabricated so that one of the sidewalls of each of the beams is coated with the cold-state reset layer. When the temperature of the device exceeds the austenite-phase temperature of the SMA, the gripper is actuated as the material returns to its remembered shape (Figure 1(b)). The shape of the gripper will be restored to be the cold-state original shape when heat is removed due to the force provided by the reset layer. The electroplating-based bonding method developed in this study (discussed in the next section) is used to achieve not only high-precision assembly of the micromachined SMA gripper on the wireless heater with high mechanical bonding strength but also high thermal conductance between the two components.

DESIGN AND FABRICATION

The SMA grippers developed have a normally closed design (Figure 2 (a)). The 4-mm-long gripper structures are formed by micro-electro-discharge machining (μEDM) [19] of 300-μm-thick Ti-Ni SMA sheets with an austenitic-phase temperature of 65 °C. The SMA components are designed to have a bonding pad with a cavity and perforations as shown in Figure 2(a). Each of the two gripper beams has a thickness of 62 μm and a compressive SiO_2 layer 3-μm thickness on the outer sidewall of the beam. This configuration is calculated to bend the beam with a displacement of ~300 μm at the tip of the beam. The spacing between the two beams at their bottoms is defined to be 570 μm so that the bending is large enough to close the gripper at its cold state. The LC circuit has a planar spiral coil with an overall size of 5×5 mm^2 and the line width and spacing as indicated in Figure 2(b). The SMA component is bonded on one of the capacitor electrodes of the LC circuit that provides heat to the SMA through the bonded region.

Figure 3 shows the process flow developed for the device fabrication. The planar LC circuit is fabricated using single-sided copper-clad polyimide (PI) film with 50-μm thickness (G2300, Shehdahl Co.). The photolithography for the circuit fabrication is performed with dry-film photoresists (MacDermid SF306 and DuPont PM240). First, one of the capacitor electrodes is formed by wet etching of the copper-clad layer (Figure 3, step 1). This electrode provides the region for the SMA bonding to the circuit. Next, the PI film is etched using a KOH-based solution to create the via contact hole in the film (Figure 3, step 2). After depositing a Ti-Cu seed layer on the PI side, copper electroplating in the patterned dry-film photoresist mold is performed to form the coil and the other capacitor electrode with a thickness of 30-35 μm (Figure 3, step 3). Figure 4(a) shows the fabricated LC circuits. For the SMA gripper fabrication, the gripper component is first shaped to have the single beam structure in a piece of the SMA sheet using μEDM. This is followed by the deposition of a 1.5-μm-thick SiO_2 layer using PECVD at 350 °C on both sides of the SMA piece so the sidewalls of the beam have ~3-μm-thick SiO_2 that serves as the reset layer. The SMA component is then μEDMed to create the bonding pad with the cavity and perforations (Figure 4(b)). This μEDM step removes the SiO_2 layer from the pad region. The bonding pad of the SiO_2-coated SMA is fixed onto the capacitive electrode on the copper-clad side of the circuit that is coated with photoresist (SPR 220-7, ROHM and HASS) (Figure 3, step 4), followed by the lithography to remove the photoresist in the pad region (Figure 3,

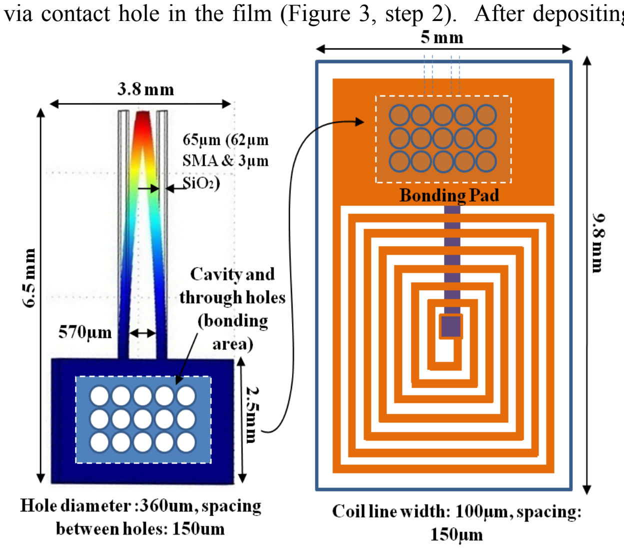

(a) (b)

Figure 2: (a) SMA gripper design and (b) LC circuit design.

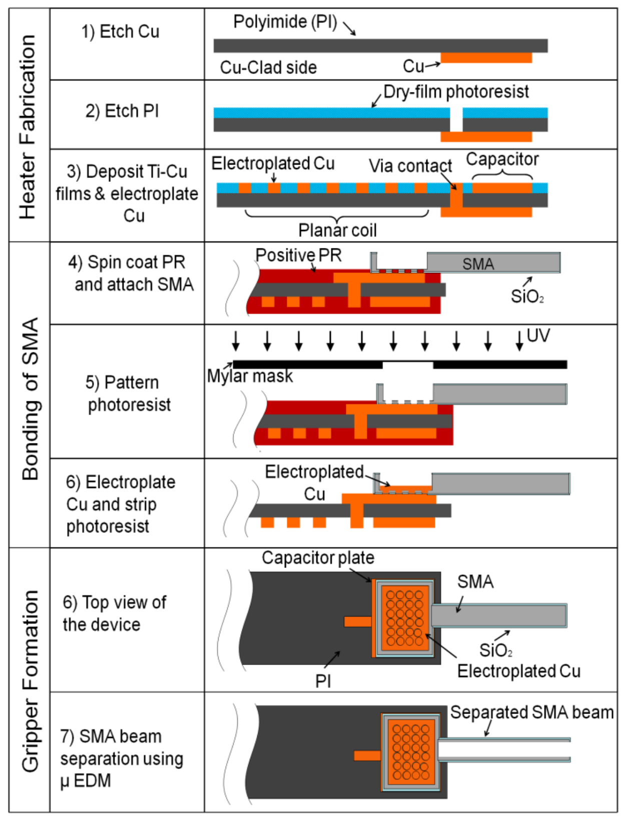

Figure 3: Fabrication process flow (cross-sectional view except steps 6 and 7).

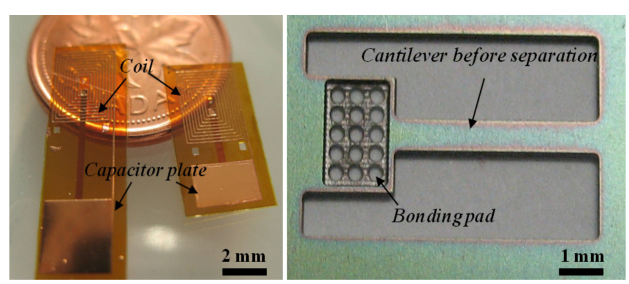

(a) (b)

Figure 4: (a) Samples of fabricated LC resonant circuits and (b) an SMA gripper component fabricate with μEDM (prior to separation from the original sheet).

step 5). Copper electroplating is then performed in the pad region (Figure 3, step 6) so that the copper grown from the capacitor electrode through the pad's perforations is over-plated and connected to the portion plated on the pad, mechanical fixing the pad. In this step, the SiO_2 layer on the SMA beam acts as a mask for electroplating so that copper is only deposited on the cavity of the SMA and on the capacitor electrode through the perforations in the cavity. Figure 6(a) shows the pad of the SMA gripper component that was bonded on the circuit with this electroplating process. Finally, the single beam of the SMA is split into two beams using μEDM (Figure 3, step 7) to form the gripper structure with vertical sidewalls (Figure 5). These split beams consequently have inner sidewalls without SiO_2 layers, resulting in bending and closing their tips due to the compressive SiO_2 layer present on the outer sidewalls of the beams. The final form of the device is shown in Figure 6 (b).

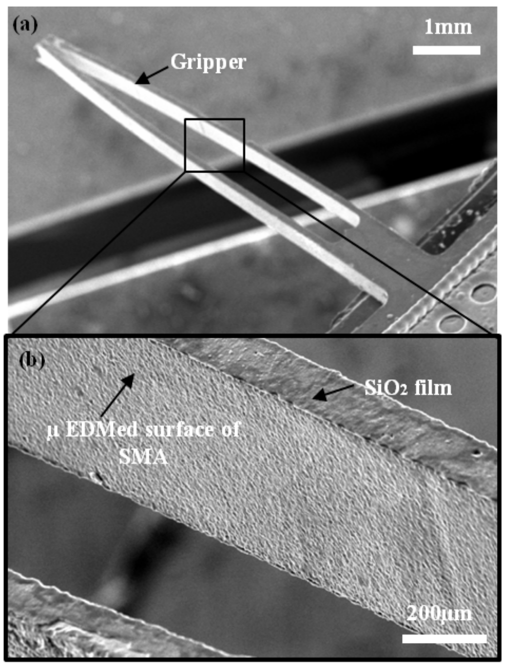

Figure 5: A fabricated SMA gripper: (a) The gripper beams split using μEDM; (b) a close- up of the inner sidewall of the beam.

EXPERIMENTAL RESULTS

Preliminary wireless tests were performed to characterize the fabricated grippers. The tests were conducted using the set-up illustrated in Figure 7. In this set-up, an amplified RF signal with an output power of up to ~1 W is fed to the external coil (diameter ~4 mm, 497-nH inductance) to generate an RF magnetic field that excites the LC circuit of the device. The thermo-mechanical behavior of the gripper was characterized using a thermocouple that was attached to the devices (on the capacitor electrode of the circuit located on the opposite side of the electrode bonded with the SMA) as well as a measuring microscope to characterize the displacement of the gripper. It was experimentally verified that the dependence of the thermocouple reading on the presence of the magnetic field with the power level and frequencies used in the tests was minimal or undetectable.

Figure 8 shows a typical thermal response of the fabricated device. The resonant frequency of the LC circuit used in this test was 105 MHz. The device temperature was measured while scanning the field frequency from 93MHz to 113MHz at a constant output power. The result shows a strong peak (of 138 °C) when the

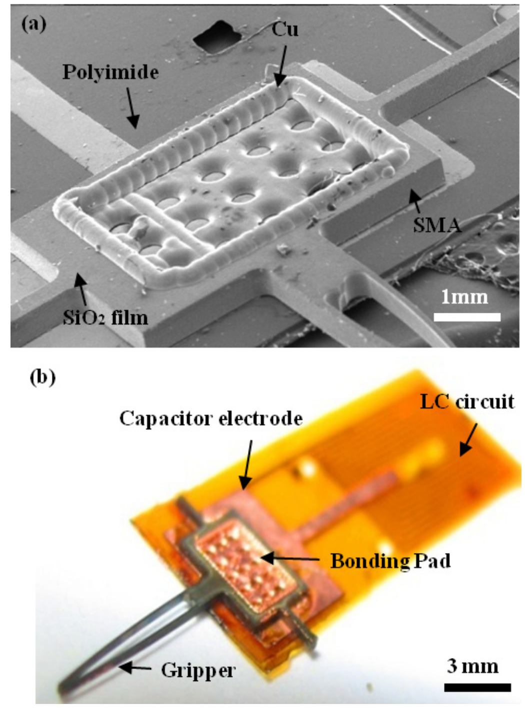

Figure 6: Fabrication results: (a) The SMA pad bonded by electroplated copper; (b) the overall shape of a fabricated device.

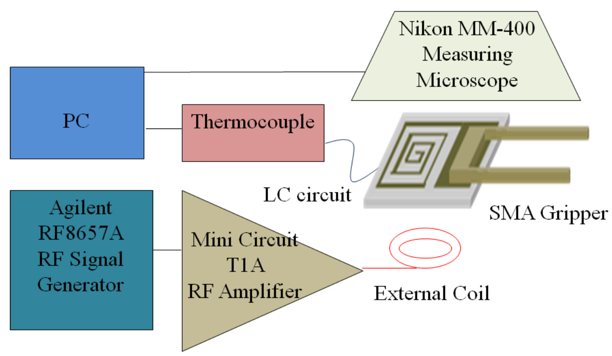

Figure 7: A set-up for wireless tests.

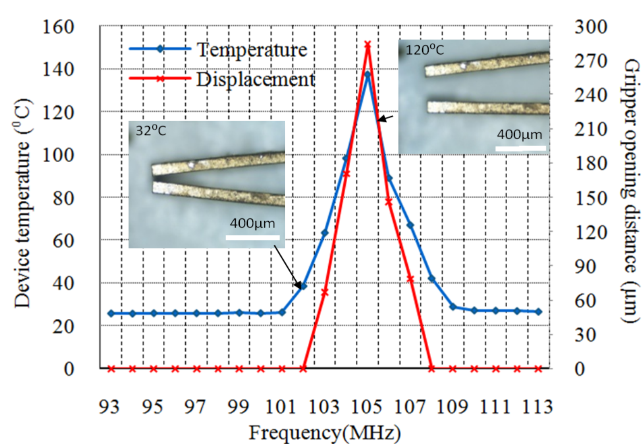

Figure 8: Measured circuit temperature and gripper openings vs. field frequency (inset images show tip opening of the gripper at corresponding temperatures).

field frequency is aligned to the resonant frequency of the circuit. The opening distance of the gripper was also measured and plotted in Figure 8, indicating the maximum opening of 290 µm. It also suggests that the actuation is initiated when the device temperature reaches around 40 °C, and that the active frequency range for the actuation of this device is ~6 MHz. The gripping ability of the devices was demonstrated using samples of vertically aligned carbon nanotube (CNT) forests as shown in Figure 9; a part of CNT forests were successfully manipulated by controlling the opening distance of the grippers fabricated in this effort.

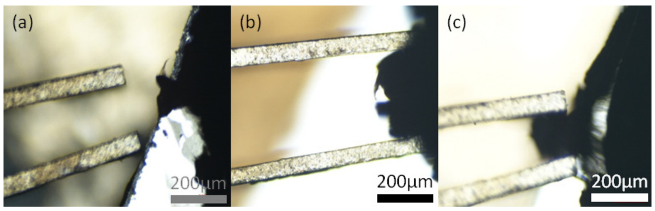

Figure 9: Manipulation of a CNT forest: (a) Approaching the forest (device temperature ~100 °C); (b) making contact (~140 °C); (c) gripping and manipulating a part of the forest (room temperature).

CONCLUSIONS

A fully passive, bulk-micromachined SMA gripper that can be controlled using external RF magnetic fields has been investigated. A 4-mm-long SMA gripper with a normally closed design was coupled with a planar resonant wireless heater with a 5×5-mm^2 spiral coil that is activated by tuning the field frequency to the resonant frequency of the heater. An electroplating-based planar bonding technique was developed to achieve mechanical and thermal coupling of the SMA gripper components with the wireless heater circuits. The fabricated grippers exhibited the tip opening of 290 µm at a device temperature of ~140 °C that was obtained when the frequency field is at the heater's resonant frequency of 105 MHz with a constant RF power of ~1 W. The frequency selectivity of the device provides an opportunity to implement simultaneous control of multiple SMA actuators that are bonded to the wireless heaters with different resonant frequencies. The developed bonding technique based on photo-defined electroplating may be leveraged for the microfabrication of arrayed SMA actuators by scaling up the technique.

ACKNOWLEDGMENTS

The authors would like to thank Ningyuan Wang for his assistance in fabrication and testing work and also Dr. Alireza Nojeh for our use of CNT forests. This work was partially supported by the Natural Sciences and Engineering Research Council of Canada, the Canada Foundation for Innovation and the British Columbia Knowledge Development Fund. M.S. Mohamed Ali acknowledges financial support from Ministry of Higher Education Malaysia and Universiti Teknologi Malaysia.

REFERENCES

[1] N.B. Morgan, "Medical shape memory alloy applications-the market and its products" Materials Science and Engineering A, vol. 378 (2004), pp. 16-23.

[2] H. Kahny, M. A. Huffz, and A. H. Heuery, "The TiNi shape-memory alloy and its applications for MEMS" J.Micromech. Microeng.: vol. 8 (1998), pp. 213-221.

[3] W. Benard, H. Kahn, A.Heuer, M. Huff, "A titanium-nickel shape-memory alloy actuated micropump", Transducers '97 Chicago, 1997, pp. 361-364 vol.1.

[4] N. Sandström, S. Braun, G. Stemme ,W. van der Wijngaart, "Full Wafer Integration of Shape Memory Alloy Microactuator using Adhesive Bonding" Proc. IEEE Transducers, 2009, pp845- 848.

[5] T. Suguwara, K. Hirota, M. Watanabe, T. Mineta, E. Makino, S. Toh and T. Shibata, "Shape memory thin film actuator for holding a fine blood vessel", Sensors and Actuators A: Physical, Vol 130-131 (2006), pp 471-467.

[6] W. M. Huang, J. P. Tan, X. Y. Gao, and J. H. Yeo, "Design, testing, and simulation of NiTi shape-memory-alloy thin-film-based microgrippers" J. Microlithography, Microfabrication, Microsystems, Vol. 2 (2003), pp 185-190.

[7] B. Kim, M.G. Lee, Y.P. Lee, Y. Kim, G. Lee, " An Earthworm-like Micro Robot using Shape Memory Alloy Actuator" Sensors and Actuators A: Physical, 125 (2) (2006), pp 429 – 437.

[8] Y.P Lee, B. Kim, M.G Lee, J.Park, "Locomotive mechanism design and fabrication of biomimetic micro robot using shape memory alloy" Proc. IEEE Robotics & Automation, 2004, pp 5007-5012.

[9] H. Kahn, M.A. Huff, A.H. Heuer, The TiNi shape-memory alloy and its applications for MEMS, Journal of Micromech. and Microeng., Vol 8 (1998), pp 213–221.

[10] Y.Q. Fu, W.M. Huang, H.J. Du, X. Huang, J.P. Tan, X.Y. Gao, Characterization of TiNi shape-memory alloy thin films for MEMS applications, Surface Coating and Technology, Vol 145 (2001), pp 107–112.

[11] A. Ishida, M. Sato, A. Takei, K. Nomura, S. Miyazaki, Effect of aging on shape memory behavior of Ti–51.3 at.% Ni thin films, Metall. Mater. Trans. A 27A (1996) pp 3753–3759.

[12] D. Reynaerts, J. Peirs and H. Brussel, "An implantable drug-delivery system based on shape memory alloy micro-actuation", Sensors and Actuators A: Physical, Volume 61, Issues 1-3 (1997), pp 455-462 .

[13] Y. Fu, H. Du, W. Huang, S. Zhang and M. Hu, "TiNi-based thin films in MEMS applications: a review", Sensors and Actuators A: Physical, vol. 112, May. 2004,.Microsyst., Vol. 2, 185 (2003), pp. 395-408.

[14] Y.Bellouard, R. Clavel, R. Gotthardt, J. E.idaux, T. Sidler, "A new concept of monolithic. Shape Memory Alloys micro-devices used in micro-robotics", Actuator'98- 6th International Conference on New Actuators, Bremen, Germany, June 17-19, 1998, P88.

[15] H. Scherngell and A.C. Kneissl, "Training and stability of the intrinsic two-way Shape memory effect in Ni-Ti alloys" Scripta Materialia. Vol 39 (1998), p. 205-212.

[16] S. Brown N. Sandström, G. Stemme, "Wafer-scale manufacturing of bulk shape-memory-alloy microactuators based on adhesive bonding of titanium-nickel sheets to structured silicon wafers" Journal of Microelectromechanical Systems, vol. 18, no 6 (2009), pp. 1309-1317

[17] E.H. Sarraf, G.K. Wong, K. Takahata, "Frequency-Selectable Wireless Actuation of Hydrogel using Micromachined Resonant Heaters Toward Implantable Drug Delivery Application" Proc. IEEE Transducers, 2009, pp 1525-1528.

[18] S.D. Senturia, *Microsystem Design*, Kluwer Academic Publishers, New York, 2001.

[19] T.Masaki, K.Kawata, T. Masuzawa, "Micro Electro-Discharge Machining and Its Applications" Proc. IEEE MEMS, 1990, pp 21-26.

CONTACT

*M.S. Mohamed Ali, tel: +1-604-761-8716;
mohamedm@ece.ubc.ca